Title: Detecting the impact of temperature on transmission of Zika, dengue and chikungunya using mechanistic models

Short title: Temperature predicts Zika, dengue, and chikungunya transmission

Authors: Erin A. Mordecai[a*], Jeremy M. Cohen[b], Michelle V. Evans[c], Prithvi Gudapati[a], Leah R. Johnson[b], Catherine A. Lippi[c], Kerri Miazgowicz[d], Courtney C. Murdock[d,e], Jason R. Rohr[b], Sadie J. Ryan[c,f,g,h], Van Savage[i,j], Marta S. Shocket[a,k], Anna Stewart Ibarra[l], Matthew B. Thomas[m], Daniel P. Weikel[n]

Affiliations:

[a]Biology Department, Stanford University, 371 Serra Mall, Stanford, CA 94305

[b]Department of Integrative Biology, University of South Florida, 4202 East Fowler Ave, SCA110 Tampa, FL 33620

[c]Department of Geography, University of Florida, PO Box 117315, Turlington Hall, Gainesville, FL 32611

[d]Center for Tropical and Emerging Global Disease, Department of Infectious Diseases, University of Georgia College of Veterinary Medicine, 501 D.W. Brooks Drive, Athens, GA 30602

[e]Odum School of Ecology, University of Georgia, 140 E. Green St., Athens, GA 30602[f]Emerging Pathogens Institute, University of Florida, P.O. Box 100009, 2055 Mowry Road Gainesville, FL 32610

[g]Center for Global Health and Translational Science, Department of Microbiology and Immunology, Weiskotten Hall, SUNY Upstate Medical University, Syracuse, NY 13210

[h]School of Life Sciences, College of Agriculture, Engineering, and Science, University of KwaZulu Natal, Private Bag X01, Scottsville, 3209, KwaZulu Natal, South Africa

[i]Department of Ecology and Evolutionary Biology, University of California Los Angeles and Department of Biomathematics, University of California Los Angeles, Los Angeles, CA 90095

[j]Santa Fe Institute, 1399 Hyde Park Rd, Santa Fe, NM 87501

[k]Department of Biology, Indiana University, 1001 E. 3rd St., Jordan Hall 142, Bloomington, IN 47405

[l]Center for Global Health and Translational Sciences, SUNY Upstate Medical University, Syracuse, NY13210

[m]Department of Entomology and Center for Infectious Disease Dynamics, Penn State University, 112 Merkle Lab, University Park, PA 16802

[n]Department of Biostatistics, University of Michigan, 1415 Washington Heights, Ann Arbor, MI 48109

[*]Correspondence to: Erin Mordecai. Biology Department, Stanford University, 371 Serra Mall, Stanford, CA 94305. (650) 497-7447. emordeca@stanford.edu

Keywords: Zika, dengue, chikungunya, temperature, vector transmission, *Aedes aegypti*, *Aedes albopictus*

Abstract

Recent epidemics of Zika, dengue, and chikungunya have heightened the need to understand the seasonal and geographic range of transmission by *Aedes aegypti* and *Ae. albopictus* mosquitoes. We use mechanistic transmission models to derive predictions for how the probability and magnitude of transmission for Zika, chikungunya, and dengue change with mean temperature, and we show that these predictions are well matched by human case data. Across all three viruses, models and human case data both show that transmission occurs between 18-34°C with maximal transmission occurring in a range from 26-29°C. Controlling for population size and two socioeconomic factors, temperature-dependent transmission based on our mechanistic model is an important predictor of human transmission occurrence and incidence. Risk maps indicate that tropical and subtropical regions are suitable for extended seasonal or year-round transmission, but transmission in temperate areas is limited to at most three months per year even if vectors are present. Such brief transmission windows limit the likelihood of major epidemics following disease introduction in temperate zones.

Main Text

Epidemics of dengue, chikungunya, and Zika are sweeping through the Americas, and are part of a global public health crisis that places an estimated 3.9 billion people in 120 countries at risk (1). Dengue virus (DENV) distribution and intensity in the Americas has increased over the last three decades, infecting an estimated 390 million people (96 million clinical) per year (2). Chikungunya virus (CHIKV) emerged in the Americas in 2013, causing 1.8 million suspected cases from 44 countries and territories (www.paho.org). In the last year, Zika virus (ZIKV) has spread throughout the Americas, causing 688,040 suspected and confirmed cases, with many more unreported (http://ais.paho.org/phip/viz/ed_zika_cases.asp, as of November 17, 2016). The growing burden of these diseases (including links between Zika infection and both microcephaly and Guillain-Barré syndrome (3)) and potential for spread into new areas creates an urgent need for predictive models that can inform risk assessment and guide interventions such as mosquito control, community outreach, and education.

Predicting transmission of DENV, CHIKV, and ZIKV requires understanding the ecology of the vector species. For these viruses the main vector is *Aedes aegypti*, a mosquito that prefers and is closely affiliated with humans, while *Ae. albopictus*, a peri-urban mosquito, is an important secondary vector (4,5). We expect one of the main drivers of the vector ecology to be the climate, particularly temperature. Along these lines, mathematical and geostatistical models that incorporate climate information have been valuable for predicting and responding to *Aedes* spp. spread and DENV, CHIKV, and ZIKV outbreaks (5–9).

The effects of temperature in ectotherms are largely predictable from fundamental metabolic and ecological processes. Survival, feeding, development, and reproductive rates predictably respond to temperature across a variety of ectotherms, including mosquitoes (10,11).

Because these traits help to determine transmission rates, the effects of temperature on transmission should also be broadly predictable from mechanistic models that incorporate temperature-dependent traits. Here, we introduce a model based on this framework that overcomes several major gaps that currently limit our understanding of climate suitability for transmission. Specifically, we develop models of temperature-dependent transmission for *Ae. aegypti* and *Ae. albopictus* that are (a) mechanistic, facilitating extrapolation beyond the current disease distribution, (b) parameterized with biologically accurate unimodal thermal responses for all mosquito and virus traits that drive transmission, and (c) validated against human dengue, chikungunya, and Zika case data across the Americas.

We synthesize available data to characterize the temperature-dependent traits of the mosquitoes and viruses that determine transmission intensity. With these thermal responses, we develop mechanistic temperature-dependent virus transmission models for *Ae. aegypti* and *Ae. albopictus*. We then ask whether the predicted effect of temperature on transmission is consistent with patterns of actual human cases over space and time. To do this, we validate the models with DENV, CHIKV, and ZIKV human incidence data at the country scale from the Americas from 2014-2016. To isolate temperature dependence, we also statistically controlled for population size and two socioeconomic factors that may influence transmission. If temperature fundamentally limits transmission potential, transmission should only occur at actual environmental temperatures that are predicted to be suitable, and conversely, areas with low predicted suitability should have low or zero transmission (i.e., false negative rates should be low). By contrast, low transmission may occur even when temperature suitability is high because other factors like vector control can limit transmission (i.e., the false positive rate should be higher than the false negative rate). Finally, if the simple mechanistic model accurately predicts

103 climate suitability for transmission, then we can use it to map climate-based transmission risk of
104 DENV, CHIKV, ZIKV, and other emerging pathogens transmitted by *Ae. aegypti* and *Ae.*
105 *albopictus* seasonally and geographically.

106 **Results**

107 *Temperature-dependent transmission*

108 Data gathered from the literature (9,12–14,14–20,20–29) revealed that all mosquito traits
109 relevant to transmission—biting rate, egg-to-adult survival and development rate, adult lifespan,
110 and fecundity—respond strongly to temperature and peak between 23°C and 34°C for the two
111 mosquito species (Figs. 1, S1). Humidity linearly increases survival at all mosquito life stages,
112 but does not interact with temperature (Fig. S2). DENV extrinsic incubation and vector
113 competence peak at 35°C (30–36) and 31-32°C (30,31,33,37), respectively, in both
114 mosquitoes—temperatures at which mosquito survival is low, limiting transmission potential
115 (Figs. 1, S1). Appropriate thermal response data were not available for CHIKV and ZIKV
116 extrinsic incubation and vector competence.

117

118 **Fig. 1.** Thermal responses of *Ae. aegypti* and DENV traits that drive transmission (data sources
119 listed in Table S2). Informative priors based on data from additional *Aedes* spp. and flavivirus
120 studies helped to constrain uncertainty in the model fits (see Materials and Methods; Table S3).
121 Points and error bars indicate the data means and standard errors (for display only; models were
122 fit from the raw data). Black solid lines are the mean model fits; red dashed lines are the 95%
123 credible intervals.

124

We estimated the posterior distribution of $R_0(T)$ and used it to calculate the mean and 95% credible intervals (95% CI) on the critical thermal minimum, maximum, and optimum temperature for transmission by the two mosquito species. At constant temperature, *Ae. aegypti* transmission peaked at 29.1°C (95% CI: 28.4 – 29.8°C), and declined to zero below 17.8°C (95% CI: 14.6 – 21.2°C) and above 34.6°C (95% CI: 34.1 – 35.6°C) (Fig. 2). *Ae. albopictus* transmission peaked at 26.4°C (95% CI: 25.2 – 27.4°C) and declined to zero below 16.2°C (95% CI: 13.2 – 19.9°C) and above 31.6°C (95% CI: 29.4 – 33.7°C) (Fig. 2). Overall, the thermal response curve for *Ae. albopictus* is shifted towards lower temperatures than *Ae. aegypti,* so *Ae. albopictus* transmission is better suited to colder environments. For a more realistic scenario in which daily temperature ranged over 8°C, the transmission peak, minimum, and maximum were slightly lower for both *Ae. aegypti* (28.5°C, 13.5°C, 34.2°C, respectively) and *Ae. albopictus* (26.1°C, 11.9°C, and 28.3°C, respectively). The lower thermal maximum under fluctuating temperatures occurs because we incorporated empirically supported irreversible lethal effects of temperatures that exceed thermal maxima for survival (see Materials and Methods).

Fig. 2. Relative R_0 across constant temperatures (°C; top) for *Ae. albopictus* (light blue lines and shading) and *Ae. aegypti* (dark blue lines and shading), and histograms of the posterior distributions of the critical thermal minimum (bottom left), temperature at peak transmission (bottom middle), and critical thermal maximum (bottom right; all in °C). Solid lines: mean posterior estimates; dashed lines: 95% credible intervals. R_0 curves normalized to a 0-1 scale for ease of comparison and visualization.

147 The posterior distribution of $R_0(T)$ allows us to evaluate uncertainty in key model
148 outcomes, including critical thermal minimum, maximum, and optimum. Uncertainty was higher
149 for the critical thermal minimum for transmission than for the maximum or optimum, and the
150 two mosquito species overlapped most for this outcome (Fig. 2, bottom panels). This occurred
151 because several trait thermal responses increase gradually from low to mid temperatures but
152 decline more steeply at high temperatures (Fig. 1), so uncertainty is greatest at low temperatures.
153 *Ae. aegypti* has a substantially higher optimum and maximum temperature than *Ae. albopictus*
154 (Fig. 2) due to its greater rates of adult survival at high temperatures (see Supplementary
155 Materials for sensitivity analyses).

156

157 *Model validation*

158 We used generalized linear models (GLM) to ask whether the predicted relationship
159 between temperature and transmission, $R_0(T)$, was consistent with observed human cases of
160 DENV, CHIKV, and ZIKV. Specifically, we assessed whether $R_0(T)$ was an important predictor
161 of the probability of autochthonous transmission occurring and of the incidence given that
162 transmission occurred. We also controlled for human population size, virus species, and two
163 socioeconomic factors. (Note that we focused on testing the $R_0(T)$ model, rather than on
164 constructing the best possible statistical model of human case data.) To do this, we used the
165 version of the *Ae. aegypti* $R_0(T)$ model that includes 8°C daily temperature range, along with
166 country-scale weekly case reports of DENV, CHIKV, and ZIKV in the Americas and the
167 Caribbean between 2014-2016. We first addressed the fact that countries with larger populations
168 have greater opportunities for (large) epidemics by creating two predictors that incorporate
169 scaled $R_0(T)$ and population size. In the models of the probability of autochthonous transmission

occurring we used the product of the posterior probability that $R_0(T) > 0$ (which we notate as GR_0) and the log of population size (p) to give $log(p)*GR_0$. In the models of incidence given that transmission does occur we used the log of the product of simple $R_0(T)$ and population size $log(p*R_0(T))$. To control for several socioeconomic factors that might obscure the impact of temperature, we also included log of gross domestic product (GDP) and log percent of GDP in tourism (using logs to improve normality). These are potential indicators of investment in and/or success of vector control and infrastructure improvements that prevent transmission. By comparing models that included the $R_0(T)$ metric alone, socioeconomic factors alone, or both, we tested whether $R_0(T)$ was an important predictor of observed transmission occurrence and incidence (see Table S4). We used both in-sample and out-of-sample analyses to assess the fit of each model, focusing on whether or not the $R_0(T)$ metric was included in each of the best models.

For the probability of autochthonous transmission occurring, the model that included both the $R_0(T)$ predictor and socioeconomic predictors had overwhelming support based on Bayesian Information Criterion (BIC; model PA5 relative probability = 1, Table S4). Based on deviance explained, the models that included $R_0(T)$, with or without the socioeconomic predictors out-performed the model that did not include $R_0(T)$ (Table S4; Figs. 3A, S3). In analyses of out-of-sample accuracy, models that included the $R_0(T)$ metric (with or without the socioeconomic factors) were surprisingly accurate. They predicted the probability of transmission with 86-91% out-of-sample accuracy for DENV (Table S4). For CHIKV and ZIKV, models that included the $R_0(T)$ metric or population alone had 66-69% out-of-sample accuracy (Table S4). There were no significant differences in out-of-sample accuracy between the top four models but for both DENV and CHIKV/ZIKV the best model was significantly better than the worst model (see Supplementary Code for full results). The lower out-of-sample accuracy for CHIKV and ZIKV

likely reflects the much lower frequency of positive values and the lower total sample size of this dataset. All results were similar for a set of models that separated GR_0 from population size, so for simplicity we show the model predictors that combines GR_0 and population size here (see Table S4 and Supplementary Code for results of other models). Together, these analyses suggest that $R_0(T)$ is an important predictor of transmission occurrence, but that CHIKV and ZIKV need further data to better explain the probability of transmission occurrence (Figs. 3A, S3).

Fig. 3. *Ae. aegypti* $R_0(T)$ and population size predict the probability and magnitude of transmission of DENV, CHIKV, and ZIKV across the Americas. A, $log(p)*GR_0$ (the posterior probability that $R_0(T) > 0$ times the log of population size) versus the probability of local transmission in the data. B, $log(p*R_0(T))$ (log of $R_0(T)$ times the population size) versus the log of incidence, given that it exceeds the threshold for local transmission. Tick-marks and points: human transmission occurrence and incidence data, respectively, by country-week in the Americas and Caribbean. Lines and shaded areas: mean and 95% CI from GLM fits for DENV (blue) and CHIKV and ZIKV (red). For simplicity, we show the models that only include the covariates $log(p)*GR_0$ or $log(p*R_0(T))$, respectively, and do not include the socioeconomic covariates (models PA6 and IM4 in Table S4). For each case report data point, $log(p)*GR_0$ and $log(p*R_0(T))$ were calculated at the mean temperature 10 weeks prior to the reporting week (38).

$R_0(T)$ was also an important predictor of incidence, given that autochthonous transmission did occur. Within-sample, incidence was best predicted by the model that included both $R_0(T)$ and the socioeconomic predictors (model IM5 in Table S4) based on BIC (relative probability = 1). The models that included $R_0(T)$ out-performed those that did not based on

deviance explained (Table S4). In out-of-sample validation, the models that included $R_0(T)$ explained the magnitude of incidence based on mean absolute percentage error (85-86% accuracy versus 83% accuracy for models that did not include $R_0(T)$; Table S4), but this difference was not statistically significant. For illustration, we show the simpler model that only contains the $R_0(T)$ predictor in the main text (Fig. 3B; model IM1 in Table S4). Notably, the models that contained $R_0(T)$ predicted incidence well for all three viruses, despite the lower incidence of CHIKV and ZIKV.

The ability of the model to explain the probability and magnitude of transmission is notable given the coarse scale of the human incidence versus mean temperature data (i.e., country-scale means), the lack of CHIKV- and ZIKV-specific trait thermal response data to inform the model, the nonlinear relationship between transmission and incidence, and all the well-documented factors other than temperature that influence transmission. Together, these analyses show simple mechanistic models parameterized with laboratory data on the two mosquito species and dengue virus are consistent with observed temperature suitability for transmission. Moreover, the similar responses of human incidence of ZIKV, CHIKV, and DENV to temperature suggest that the thermal ecology of their shared mosquito vectors is a key determinant of outbreak location, timing, and intensity.

Mapping climate suitability for transmission

The validated model can be used to predict where transmission is not excluded (posterior probability that $R_0(T) > 0$, a conservative estimate of transmission risk). Considering the number of months per year at which mean temperatures do not prevent transmission, large areas of tropical and subtropical regions, including Puerto Rico and parts of Florida and Texas, are

currently suitable year-round or seasonally (Fig. 4). These regions are fundamentally at risk for DENV, CHIKV, ZIKV, and other *Aedes* arbovirus transmission during a substantial part of the year (Fig. 4). Indeed, DENV, CHIKV, and/or ZIKV local transmission has occurred in Texas, Florida, Hawaii, and Puerto Rico (www.cdc.gov). On the other hand, many temperate regions experience temperatures suitable for transmission three months or less per year (Fig. 4), and the virus incubation periods in humans and mosquitoes restrict the transmission window even further. Temperature thus limits the potential for the viruses to generate extensive epidemics in temperate areas even where the vectors are present. Moreover, many temperate regions with seasonally suitable temperatures currently lack *Ae. aegypti* and *Ae. albopictus* mosquitoes, making vector transmission impossible (Fig. 4, black line). The posterior distribution of $R_0(T)$ also allows us to map months of risk with different degrees of uncertainty (e.g., 97.5%, 50%, and 2.5% posterior probability that that $R_0 > 0$), ranging from the most to least conservative (Fig. S5).

Fig. 4. Map of predicted temperature suitability for virus transmission by *Ae. albopictus* and *Ae. aegypti*. Color indicates the consecutive months in which temperature is permissive for transmission (predicted $R_0 > 0$) for *Aedes* spp. transmission based on the minimum likely range (> 97.5% posterior probability that $R_0 > 0$). Black line indicates the CDC estimated range for the two *Aedes* spp. in the United States. Model suitability predictions combine temperature mean and 8°C daily variation and are informed by laboratory data (Figs. 1, S1) and validated against field data (Fig. 3).

Discussion

Temperature is an important driver of—and limitation on—vector transmission, so accurately describing the temperature range and optimum for transmission of DENV, CHIKV, and ZIKV is critical for predicting their geographic and seasonal patterns of spread. We directly estimated the temperature – transmission relationship using mechanistic transmission models for each mosquito species (Fig. 2). These models are built using empirical estimates of the (unimodal) effects of temperature on mosquito and pathogen traits that drive transmission, including survival, development, reproduction, and biting rates (Figs. 1, S1). Because these trait thermal responses are unimodal across the majority of ectotherm taxa and traits, and because the traits combine nonlinearly to drive transmission, the emergent relationship between temperature and transmission is difficult to infer directly from field data or from individual trait responses. Here, we present a model of temperature-dependent DENV, CHIKV, and ZIKV transmission that advances on previous models because it is mechanistic, fitted from experimental trait data, and validated against human case data at a broad geographic scale (Fig. 3). This mechanistic understanding is valuable for extrapolating beyond the current spatial and temporal range of transmission (Fig. 4). Of the four previous mechanistic temperature-dependent *Ae. aegypti* DENV or CHIKV transmission models we were able to reproduce, our model has a similar optimum but higher critical thermal maximum than two of the models (39,40), and declines much more steeply at high temperatures than two other models (7,9) (Fig. S6).

Even though the thermal response data are imperfect—for example, CHIKV and ZIKV thermal response data are missing—and the human case data are reported at a coarse spatial scale, the validation analyses suggest that $R_0(T)$ is an important predictor of both the probability of transmission occurring and the magnitude of incidence for DENV, CHIKV, and ZIKV. This has several key implications. First, temperature-dependent transmission is pervasive enough to

be detected at a coarse spatial scale. Second, dynamics of the mosquito predict transmission for a suite of *Ae. aegypti*-transmitted viruses, without additional virus-specific information. Third, climate and socio-economic factors combine to shape variation in incidence across countries. Finally, these simple predictors explain a substantial proportion of the variance in both the probability and intensity of transmission.

Predicting arbovirus transmission at a higher spatial resolution and precision will require more detailed information on factors like the exposure and susceptibility of human populations, environmental variation (e.g., oviposition habitat availability, seasonal and daily temperature variation), and socioeconomic factors. However, as a first step our mechanistic model provides valuable insight because it makes broad predictions about suitable environmental conditions for transmission, it is mechanistic and grounded in experimental trait data, it is validated against human case data, and its predictions are applicable across three different viruses. Using these thermal response models as a scaffold, additional drivers could be incorporated to obtain more precise and specific predictions about transmission dynamics, which could in turn be used for public health and vector control applications. For this purpose, all code and data used in the models are available as Supplementary Files.

The socio-ecological conditions that enabled CHIKV, ZIKV, and DENV to become the three most important emerging vector-borne diseases in the Americas make the emergence of additional *Aedes*-transmitted viruses likely (potentially including Rift Valley fever, yellow fever, Uganda S, or Ross River viruses). Efforts to extrapolate and to map temperature suitability (Fig. 4) will be critical for improving management of both ongoing and future emerging epidemics. Mechanistic models like the one presented here are useful for extrapolating the potential geographic range of transmission beyond the current envelope of environmental conditions in

which transmission occurs (e.g., under climate change and for newly invading pathogens). Accurately estimating temperature-driven transmission risk in both highly suitable and marginal regions is critical for predicting and responding to future outbreaks of these and other *Aedes*-transmitted viruses.

Materials and Methods

Temperature-sensitive R_0 models

We constructed temperature-dependent models of transmission using a previously developed R_0 framework. We modeled transmission rate as the basic reproduction rate, R_0—the number of secondary infections that would originate from a single infected individual introduced to a fully susceptible population. In previous work on malaria, we adapted a commonly used expression for R_0 for vector transmission to include the temperature-sensitive traits that drive mosquito population density (11):

$$R_0(T) = \left(\frac{a(T)^2\, b(T)\, c(T)\, e^{-\mu(T)/PDR(T)}\, EFD(T)\, p_{EA}(T)\, MDR(T)}{N\, r\, \mu(T)^3}\right)^{1/2} \quad (1)$$

Here, (T) indicates that the trait is a function of temperature, T; a is the per-mosquito biting rate, b is the proportion of infectious bites that infect susceptible humans, c is the proportion of bites on infected humans that infect previously uninfected mosquitoes (i.e., $b*c$ = vector competence), μ is the adult mosquito mortality rate (lifespan, $lf = 1/\mu$), PDR is the parasite development rate (i.e., the inverse of the extrinsic incubation period, the time required between a mosquito biting an infected host and becoming infectious), EFD is the number of eggs produced per female mosquito per day, p_{EA} is the mosquito egg-to-adult survival probability, MDR is the mosquito immature development rate (i.e., the inverse of the egg-to-adult development time), N is the density of humans, and r is the human recovery rate. For each temperature-sensitive trait in each

mosquito species, we fit either symmetric (Quadratic, $-c(T - T_0)(T - T_m)$) or asymmetric (Brière, $cT(T - T_0)(T_m - T)^{1/2}$) unimodal thermal response models to the available empirical data (41). In both functions, T_0 and T_m are respectively the minimum and maximum temperature for transmission, and c is a positive rate constant.

We consider a relativized version of the R_0 equation because absolute values of R_0 depend on additional factors not captured in our model. Therefore, $R_0 > 0$ is an absolute threshold for whether or not transmission is possible, but the model does not predict when transmission is stable (i.e., absolute $R_0 > 1$). While absolute estimates of R_0 are difficult to obtain and different model formulations can produce different results, our use of relative R_0 adequately describes the nonlinear relationship between mosquito and virus traits and transmission. Different expressions for R_0, including the square of equation (1), map monotonically onto our function, so they produce identical estimates for the points at which transmission declines to zero and peaks.

We fit the trait thermal responses in equation (1) based on an exhaustive search of published laboratory studies that fulfilled the criterion of measuring a trait at three or more constant temperatures, ideally capturing both the rise and the fall of each unimodal curve (Tables S1-S2). Constant-temperature laboratory conditions are required to isolate the direct effect of temperature from confounding factors in the field and to provide a baseline for estimating the effects of temperature variation through rate summation (42). We attempted to obtain raw data from each study, but if they were not available we collected data by hand from tables or digitized data from figures using WebPlotDigitizer (43). We obtained raw data from Delatte (18) and Alto (20) for the *Ae. albopictus* egg-to-adult survival probability (*pEA*), mosquito development rate (MDR), gonotrophic cycle duration (GCD, which we assumed was equal to the inverse of the

biting rate) and total fecundity (TFD) (Table S2). Data did not meet the inclusion criterion for CHIKV or ZIKV vector competence (*b, c*) or extrinsic incubation period (*EIP*) in either *Ae. albopictus* or *Ae. aegypti*. Instead, we used DENV EIP and vector competence data, combined with sensitivity analyses.

Following Johnson *et al.* (44), we fit a thermal response for each trait using Bayesian models. We first fit Bayesian models for each trait thermal response using uninformative priors ($T_0 \sim$ Uniform (0, 24), $T_m \sim$ Uniform (25, 45), $c \sim$ Gamma (1, 10) for Brière and $c \sim$ Gamma (1, 1) for Quadratic fits) chosen to restrict each parameter to its biologically realistic range (i.e., $T_0 < T_m$ and we assumed that temperatures below 0°C and above 45°C were lethal). Any negative values for all thermal response functions were truncated at zero, and thermal responses for probabilities (p_{EA}, *b,* and *c*) were also truncated at one. We modeled the observed data as arising from a normal distribution with the mean predicted by the thermal response function calculated at the observed temperature, and the precision τ, ($\tau = 1/\sigma$), distributed as $\tau \sim$ Gamma (0.0001, 00001). We fit the models using Markov Chain Monte Carlo (MCMC) sampling in JAGS, using the R (45) package *rjags* (46). For each thermal response, we ran five MCMC chains with a 5000-step burn-in and saved the subsequent 5000 steps. We thinned the posterior samples by saving every fifth sample and used the samples to calculate R_0 from 15-40°C, producing a posterior distribution of R_0 versus temperature. We summarized the relationship between temperature and each trait or overall R_0 by calculating the mean and 95% highest posterior density interval (HPD interval; a type of credible interval that includes the smallest continuous range containing 95% of the probability, as implemented in the *coda* package (47)) for each curve across temperatures.

We fit a second set of models for each mosquito species that used informative priors to reduce uncertainty in R_0 versus temperature and in the trait thermal responses. In these models, we used Gamma-distributed priors for each parameter T_0, T_m, c, and τ fit from an additional 'prior' dataset of *Aedes* spp. trait data that did not meet the inclusion criteria for the primary dataset (Table S3). We found that these initial informative priors could have an overly strong influence on the posteriors, in some cases drawing the posterior distributions well away from the primary dataset, which was better controlled and met the inclusion criteria. We accounted for our lower confidence in this data set by increasing the variance in the informative priors, by multiplying all hyperparameters (i.e., the parameters of the Gamma distributions of priors for T_0, T_m, and c) by a constant k to produce a distribution with the same mean but $1/k$ times larger variance. We chose the value of k based on our relative confidence in the prior versus main data. Thus we chose $k = 0.5$ for b, c, and PDR and $k = 0.01$ for lf. This is the main model presented in the text (Fig. 2). It is comparable to some but not all previous mechanistic models for *Ae. aegypti* and *Ae. albopictus* transmission (Fig. S6). Results of our main model, fit with informative priors, did not vary substantially from the model fit with uninformative priors (Figs. S7-S8).

Effects of humidity on dengue R_0

Like temperature, humidity is expected to affect vector transmission via its effects on mosquito populations. Specifically, we expected humidity to affect egg-to-adult survival and adult survival. Using the methods described above, we extracted experimental laboratory data on these traits measured at a range of constant humidities in the laboratory. We searched for *Aedes* spp. survival probability data across temperature and humidity. We obtained data on *Aedes aegypti* egg hatching probability (48) and *Anopheles gambiae* lifespan (49), which we used in absence of *Aedes* spp. because they have a similar (tropical, anthrophilic) life history. We used

linear regression to estimate the relationship between these traits and relative humidity (%), plugged them into the $R_0(T)$ equation (assuming the probability of egg hatching and egg-to-adult survival have the same relationship with humidity), and plotted R_0 versus temperature across a range of relative humidity values (Fig. S2). For the dataset that included variation in temperature and humidity independently, there was no interaction between the unimodal temperature response and the linear humidity response (i.e., humidity did not affect the relationship between lifespan and temperature) (49). The resulting relationship between R_0 and relative humidity was exponential. Humidity is not included in the main models presented in the text.

Incorporating daily temperature variation in transmission models

Because organisms do not typically experience constant temperature environments in nature, we incorporated the effects of temperature variation on transmission by calculating a daily average R_0 assuming a daily temperature range of 8°C, across a range of mean temperatures. This range is consistent with daily temperature variation in tropical and subtropical environments but lower than in most temperate environments. At each mean temperature, we used a Parton-Logan model to generate hourly temperatures and calculate each temperature-sensitive trait on an hourly basis (50). We assumed an irreversible high-temperature threshold above which mosquitoes die and transmission is impossible (51,52). We set this threshold based on hourly temperatures exceeding the critical thermal maximum (T_m in Tables S1-S2) for egg-to-adult survival or adult longevity by any amount for five hours or by 3°C for one hour. We averaged each trait over 24 hours to obtain a daily average trait value, which we used to calculate relative R_0 across a range of mean temperatures. We used this model in the validation against human cases (Fig. 3) and the risk map (Fig. 4).

Model validation with DENV, CHIKV, and ZIKV incidence data

To validate the model, we used data on human cases of DENV, CHIKV, and ZIKV at the country scale and mean temperature during the transmission window. Using statistical models (as described below), we estimated the effects of predicted $R_0(T)$ on the probability of local transmission and the magnitude of incidence, controlling for population size and several socioeconomic factors. We downloaded and manually entered Pan American Health Organization (PAHO) weekly case reports for DENV and CHIKV for all countries in the Americas (North, Central, and South America and the Caribbean Islands) from week 1 of 2014 to week 8 of 2015 for CHIKV and from week 52 of 2013 to week 47 of 2015 for DENV (www.paho.org). ZIKV weekly case reports for reporting districts (e.g., provinces) within Colombia, Mexico, El Salvador, and the US Virgin Islands were available from the CDC Epidemic Prediction Initiative (https://github.com/cdcepi/) from November 28, 2015 to April 2, 2016. We aggregated the ZIKV data into country-level weekly case reports to match the spatial resolution of the DENV, CHIKV, and covariate data.

Temperature data collection

We matched the DENV, CHIKV, and ZIKV incidence data with temperature using daily temperature data from METAR stations in each country, averaged at the country level by epidemic week. A previous study found a six-week lagged relationship between temperature and oviposition for *Aedes aegypti* in Ecuador (38). Assuming that the subsequent transmission, disease development, medical care-seeking, and case reporting in humans takes an additional four weeks, we assumed *a priori* a ten-week lag between temperature and incidence (i.e., mean temperature for the week that is ten weeks prior to each case report). METAR stations are internationally standardized weather reporting stations that report hourly temperature and

444 precipitation measures. Outlier weather stations were excluded if they reported a daily maximum
445 temperature below 5°C or a daily minimum temperature above 40°C during the study period,
446 extremes that would certainly eliminate the potential for transmission in a local area. Because
447 case data are reported at the country level, we needed a collection of weather stations in each
448 country that accurately represent weather conditions in the areas where transmission occurs,
449 excluding extreme areas where transmission is unlikely. For the study period of October 1, 2013
450 through April 30, 2016, we downloaded daily temperature data for each station from Weather
451 Underground using the *weatherData* package in R (53). We removed all data from Chile because
452 it spans so much latitude and the terrain is so diverse that its country-level mean is unlikely to be
453 very representative of the temperature where an outbreak occurred.

454 Socioeconomic covariate data

455 We accessed available data on projected 2016 gross domestic product (GDP) for
456 countries of interest via the International Monetary Fund's World Economic Outlook Database
457 (http://www.imf.org/external/ns/cs.aspx?id=28). The direct and total contributions of tourism to
458 GDP in 2016 were compiled from World Travel and Tourism Council economic impact reports
459 (http://www.wttc.org/research/economic-research/economic-impact-analysis/country-
460 reports/#undefined). We retrieved population size data for 2013-2015 from the United Nations
461 Population Division (https://esa.un.org/unpd/wpp/Download/Standard/Population/) and averaged
462 them across the three years for each country.

463 Validation analyses with human incidence versus temperature datasets

464 To validate the $R_0(T)$ model while controlling for population and socio-economic factors,
465 we used generalized linear regression on the weekly case count data. Importantly, we focused on
466 testing whether the case counts were consistent with the transmission – temperature relationship

predicted from our model, rather than on maximizing the variation explained in the statistical model. We are more specifically interested in understanding autochthonous transmission (i.e., locally acquired, not just imported cases). We set country-level thresholds for the number of cases defining autochthonous transmission for our three diseases separately, based on current transmission understanding: seven cases of CHIKV, 70 cases of DENV, and three cases of ZIKV. The resulting data consisted of zeros for no transmission and positive case counts when transmission is presumed to be occurring. To model these data, we used a hurdle model that first uses logistic regression on the presence/absence of local transmission data to understand the factors correlated with local transmission occurring or not (PA analysis). Then we modeled the log of incidence (number of new cases per reporting week) for positive values with a gamma generalized linear models (GLM; i.e., incidence analysis).

We were interested in understanding whether $R_0(T)$ was an important predictor of human transmission occurrence and incidence, after controlling for potentially confounding factors like population size and socioeconomic conditions. To do this, we fit a series of models with different subsets of predictors that included $R_0(T)$, the socioeconomic variables with population, or both (see Table S4 for full models). To control for human population size, we created new metrics based on $R_0(T)$ and population size to use for validation against the PAHO incidence data. We define GR_0, which is the posterior probability that $R_0(T) > 0$. We use $log(p)*GR_0$, where p is the population size, as the relevant R_0-based predictor for the PA analysis. For the incidence analysis, we instead use $log(p*R_0(T))$ as the predictor. In all cases log refers to the natural logarithm. For simplicity, we refer to these as the $R_0(T)$ metrics hereafter and in the Results.

In both the PA and incidence analyses, we first used the full data sets to examine which of the candidate models best described the data. Randomized quantile residuals indicated that the

logistic and gamma GLM models were performing adequately. We compared the approximate model probabilities, calculated from the BIC scores, as well as the proportion of deviance explained (D^2) from each model. Next we examined the performance of the models in predicting out of sample, for both PA and incidence analyses. To do this we created 1000 random partitions, where 90% of the data were used to train the model and 10% were used for testing. In the PA analyses we classified each partition based on presence/absence, with separate classification thresholds for DENV versus CHIKV/ZIKV as these grouping had much different probabilities of occurrence. We assessed the performance of the model for the PA analysis based on the mean misclassification rate. In the incidence analyses we assessed the model performance based on the predictive mean absolute percentage error (MAPE). Since differences in prediction success between the models in both the PA and incidence analyses were not statistically significant, we present the simpler models that only include the $R_0(T)$ metrics in the main text (Fig. 3) and the models that additionally include socioeconomic covariates in the Supplementary Information (Figs. S3-S4). We plotted the model predictions as a function of the $R_0(T)$ metrics together with the observed data for the PA and incidence analyses using the R package *visreg* (54).

Mapping temperature suitability for transmission

Using our validated model, we were interested in where the temperature was suitable for *Ae. aegypti* and/or *Ae. albopictus* transmission for some or all of the year to predict the potential geographic range of outbreaks in the Americas. We visualized the minimum, median, and maximum extent of transmission based on probability of occurrence thresholds from the R_0 models for both mosquitoes. We calculated the number of consecutive months in which the posterior probability of $R_0 > 0$ exceeds a threshold of 0.025, 0.5, or 0.975 for both mosquito

species, representing the maximum, median, and minimum likely ranges, respectively. The minimum range is shown in Fig. 4 and all three ranges are overlaid in Fig. S5. This analysis indicates the predicted seasonality of temperature suitability for transmission geographically, but does not indicate its magnitude. To generate the maps, we cropped monthly mean temperature rasters from 1950-2000 for all twelve months (Worldclim; www.worldclim.org/) to the Americas (*R*, *raster* package, *crop* function) and assigned cells values of 1 or 0 depending on whether the probability that $R_0 > 0$ exceeded the threshold at the temperatures in those cells (Table S3). We then synthesized the monthly grids into a single raster that reflected the maximum number of consecutive months where cell values equaled 1. The resulting rasters were plotted in ArcGIS 10.3, overlaying the three cutoffs (Figure 3). We repeated this process for both mosquito species.

Acknowledgments

Barry Alto, Krijn Paaijmans, Francis Ezeakacha, and Helene Delatte kindly provided raw data used in the analyses. We gratefully acknowledge the Centers for Disease Control and Prevention Epidemic Predictions Initiative (CDC EPI) for collating and sharing the Zika incidence data on GitHub (https://zenodo.org/record/48946#.Vz-EM2bb8ys). The authors declare no competing interests.

Author contributions:

EAM, MBT, VS, SJR, LRJ, ASI, and JRR designed the research. JMC, MVE, PG, CAL, KM, CCM, MSS, DPW, and EAM conducted the research. EAM wrote the first draft of the paper and all authors contributed to revisions.

References:

1. Brady OJ, Gething PW, Bhatt S, Messina JP, Brownstein JS, Hoen AG, et al. Refining the global spatial limits of dengue virus transmission by evidence-based consensus. PLOS Negl Trop Dis. 2012 Aug 7;6(8):e1760.

2. Bhatt S, Gething PW, Brady OJ, Messina JP, Farlow AW, Moyes CL, et al. The global distribution and burden of dengue. Nature. 2013 Apr 25;496(7446):504–7.

3. Rasmussen SA, Jamieson DJ, Honein MA, Petersen LR. Zika virus and birth defects — reviewing the evidence for causality. N Engl J Med. 2016 Apr 13;374:1981–7.

4. Scott TW, Takken W. Feeding strategies of anthropophilic mosquitoes result in increased risk of pathogen transmission. Trends Parasitol. 2012 Mar;28(3):114–21.

5. Messina JP, Kraemer MU, Brady OJ, Pigott DM, Shearer FM, Weiss DJ, et al. Mapping global environmental suitability for Zika virus. eLife. 2016 Apr 19;5:e15272.

6. Magori K, Legros M, Puente ME, Focks DA, Scott TW, Lloyd AL, et al. Skeeter Buster: A stochastic, spatially explicit modeling tool for studying Aedes aegypti population replacement and population suppression strategies. PLOS Negl Trop Dis. 2009 Sep 1;3(9):e508.

7. Johansson MA, Powers AM, Pesik N, Cohen NJ, Staples JE. Nowcasting the spread of chikungunya virus in the Americas. PLoS ONE. 2014 Aug 11;9(8):e104915.

8. Perkins TA, Metcalf CJE, Grenfell BT, Tatem AJ. Estimating drivers of autochthonous transmission of chikungunya virus in its invasion of the Americas. PLoS Curr [Internet]. 2015 Feb 10 [cited 2015 Aug 18];7. Available from: http://www.ncbi.nlm.nih.gov/pmc/articles/PMC4339250/

9. Morin CW, Monaghan AJ, Hayden MH, Barrera R, Ernst K. Meteorologically driven simulations of dengue epidemics in San Juan, PR. PLoS Negl Trop Dis. 2015 Aug 14;9(8):e0004002.

10. Dell AI, Pawar S, Savage VM. Systematic variation in the temperature dependence of physiological and ecological traits. Proc Natl Acad Sci. 2011 May 23;108(26):10591–6.

11. Mordecai EA, Paaijmans KP, Johnson LR, Balzer CH, Ben-Horin T, de Moor E, et al. Optimal temperature for malaria transmission is dramatically lower than previously predicted. Ecol Lett. 2013;16:22–30.

12. Focks DA, Haile DG, Daniels E, Mount GA. Dynamic life table model for Aedes aegypti (Diptera: Culicidae): analysis of the literature and model development. J Med Entomol. 1993 Nov;30(6):1003–17.

13. Yang HM, Macoris MLG, Galvani KC, Andrighetti MTM, Wanderley DMV. Assessing the effects of temperature on the population of Aedes aegypti, the vector of dengue. Epidemiol Infect. 2009;137(08):1188–202.

14. Rueda L, Patel K, Axtell R, Stinner R. Temperature-dependent development and survival rates of Culex quinquefasciatus and Aedes aegypti (Diptera: Culicidae). J Med Entomol. 1990;27(5):892–8.

15. Tun-Lin W, Burkot TR, Kay BH. Effects of temperature and larval diet on development rates and survival of the dengue vector Aedes aegypti in north Queensland, Australia. Med Vet Entomol. 2000 Mar 1;14(1):31–7.

16. Kamimura K, Matsuse IT, Takahashi H, Komukai J, Fukuda T, Suzuki K, et al. Effect of temperature on the development of Aedes aegypti and Aedes albopictus. Med Entomol Zool. 2002;53(1):53–8.

17. Eisen L, Monaghan AJ, Lozano-Fuentes S, Steinhoff DF, Hayden MH, Bieringer PE. The impact of temperature on the bionomics of Aedes (Stegomyia) aegypti, with special reference to the cool geographic range margins. J Med Entomol. 2014 May 1;51(3):496–516.

18. Delatte H, Gimonneau G, Triboire A, Fontenille D. Influence of temperature on immature development, survival, longevity, fecundity, and gonotrophic cycles of Aedes albopictus, vector of chikungunya and dengue in the Indian Ocean. J Med Entomol. 2009 Jan 1;46(1):33–41.

19. Muturi EJ, Lampman R, Costanzo K, Alto BW. Effect of temperature and insecticide stress on life-history traits of Culex restuans and Aedes albopictus (Diptera: Culicidae). J Med Entomol. 2011 Mar;48(2):243–50.

20. Alto BW, Juliano SA. Temperature effects on the dynamics of Aedes albopictus (Diptera: Culicidae) populations in the laboratory. J Med Entomol. 2001 Jul;38(4):548–56.

21. Westbrook CJ, Reiskind MH, Pesko KN, Greene KE, Lounibos LP. Larval environmental temperature and the susceptibility of Aedes albopictus Skuse (Diptera: Culicidae) to chikungunya virus. Vector-Borne Zoonotic Dis. 2010 Apr 28;10(3):241–7.

22. Briegel H, Timmermann SE. Aedes albopictus (Diptera: Culicidae): Physiological aspects of development and reproduction. J Med Entomol. 2001 Jul 1;38(4):566–71.

23. Calado DC, Navarro-Silva MA. Influência da temperatura sobre a longevidade, fecundidade e atividade hematofágica de Aedes (Stegomyia) albopictus Skuse, 1894 (Diptera, Culicidae) sob condições de laboratório. Rev Bras Entomol. 2002;46(1):93–8.

24. Beserra EB, Fernandes CRM, Silva SA de O, Silva LA da, Santos JW dos. Efeitos da temperatura no ciclo de vida, exigências térmicas e estimativas do número de gerações anuais de Aedes aegypti (Diptera, Culicidae). Iheringia Sér Zool [Internet]. 2009 [cited 2015 Sep 10]; Available from: http://agris.fao.org/agris-search/search.do?recordID=XS2010500501

25. Westbrook CJ. Larval ecology and adult vector competence of invasive mosquitoes Aedes albopictus and Aedes aegypti for Chikungunya virus [Internet]. University of Florida; 2010 [cited 2013 Oct 23]. Available from: http://etd.fcla.edu/UF/UFE0041830/westbrook_c.pdf

26. Couret J, Dotson E, Benedict MQ. Temperature, Larval Diet, and Density Effects on Development Rate and Survival of Aedes aegypti (Diptera: Culicidae). PLoS ONE. 2014 Feb 3;9(2):e87468.

27. Ezeakacha N. Environmental impacts and carry-over effects in complex life cycles: the role of different life history stages. Dissertation [Internet]. 2015 Dec 11; Available from: http://aquila.usm.edu/dissertations/190

28. Teng H-J, Apperson CS. Development and Survival of Immature Aedes albopictus and Aedes triseriatus (Diptera: Culicidae) in the Laboratory: Effects of Density, Food, and Competition on Response to Temperature. J Med Entomol. 2000 Jan 1;37(1):40–52.

29. Wiwatanaratanabutr S, Kittayapong P. Effects of temephos and temperature on Wolbachia load and life history traits of Aedes albopictus. Med Vet Entomol. 2006;20(3):300–307.

30. Xiao F-Z, Zhang Y, Deng Y-Q, He S, Xie H-G, Zhou X-N, et al. The effect of temperature on the extrinsic incubation period and infection rate of dengue virus serotype 2 infection in Aedes albopictus. Arch Virol. 2014 Jul 3;159(11):3053–7.

31. Watts DM, Burke DS, Harrison BA, Whitmire RE, Nisalak A. Effect of temperature on the vector efficiency of Aedes aegypti for dengue 2 virus. Am J Trop Med Hyg. 1987 Jan;36(1):143–52.

32. McLean DM, Clarke AM, Coleman JC, Montalbetti CA, Skidmore AG, Walters TE, et al. Vector capability of Aedes aegypti mosquitoes for California encephalitis and dengue viruses at various temperatures. Can J Microbiol. 1974 Feb 1;20(2):255–62.

33. Carrington LB, Armijos MV, Lambrechts L, Scott TW. Fluctuations at a low mean temperature accelerate dengue virus transmission by Aedes aegypti. PLoS Negl Trop Dis. 2013 Apr 25;7(4):e2190.

34. Davis NC. The effect of various temperatures in modifying the extrinsic incubation period of the yellow fever virus in Aedes aegypti. Am J Epidemiol. 1932 Jul 1;16(1):163–76.

35. McLean DM, Miller MA, Grass PN. Dengue virus transmission by mosquitoes incubated at low temperatures. Mosq News [Internet]. 1975 [cited 2015 Aug 26]; Available from: http://agris.fao.org/agris-search/search.do?recordID=US19760088008

36. Focks DA, Daniels E, Haile DG, Keesling JE. A simulation model of the epidemiology of urban dengue fever: literature analysis, model development, preliminary validation, and samples of simulation results. Am J Trop Med Hyg. 1995 Nov;53(5):489–506.

37. Alto BW, Bettinardi D. Temperature and dengue virus infection in mosquitoes: independent effects on the immature and adult stages. Am J Trop Med Hyg. 2013 Mar;88(3):497–505.

38. Stewart Ibarra AM, Ryan SJ, Beltrán E, Mejía R, Silva M, Muñoz Á. Dengue vector dynamics (Aedes aegypti) influenced by climate and social factors in Ecuador: implications for targeted control. PLoS ONE. 2013 Nov 12;8(11):e78263.

39. Wesolowski A, Qureshi T, Boni MF, Sundsøy PR, Johansson MA, Rasheed SB, et al. Impact of human mobility on the emergence of dengue epidemics in Pakistan. Proc Natl Acad Sci. 2015 Sep 8;201504964.

40. Liu-Helmersson J, Stenlund H, Wilder-Smith A, Rocklöv J. Vectorial Capacity of Aedes aegypti: Effects of Temperature and Implications for Global Dengue Epidemic Potential. PLoS ONE. 2014 Mar 6;9(3):e89783.

41. Briere J-F, Pracros P, Le Roux A-Y, Pierre J-S. A novel rate model of temperature-dependent development for arthropods. Environ Entomol. 1999 Feb 1;28(1):22–9.

42. Lambrechts L, Paaijmans KP, Fansiri T, Carrington LB, Kramer LD, Thomas MB, et al. Impact of daily temperature fluctuations on dengue virus transmission by Aedes aegypti. Proc Natl Acad Sci. 2011 May 3;108(18):7460–5.

43. Rohatgi A. WebPlotDigitizer [Internet]. 2015. Available from: http://arohatgi.info/WebPlotDigitizer

44. Johnson LR, Ben-Horin T, Lafferty KD, McNally A, Mordecai E, Paaijmans KP, et al. Understanding uncertainty in temperature effects on vector-borne disease: a Bayesian approach. Ecology. 2015 Jan 1;96(1):203–13.

45. R Development Core Team. R: A Language and Environment for Statistical Computing [Internet]. Vienna, Austria: R Foundation for Statistical Computing; 2014. Available from: http://www.R-project.org

46. Plummer M. rjags: Bayesian Graphical Models using MCMC [Internet]. 2016. Available from: http://CRAN.R-project.org/package=rjags

47. Plummer M, Best N, Cowles K, Vines K. CODA: Convergence Diagnosis and Output Analysis for MCMC. 2006. (R News).

48. Dickerson CZ. The effects of temperature and humidity on the eggs of Aedes aegypti (L.) and Aedes albopictus (skuse) in Texas [Doctoral]. [College Station, Texas]: Texas A & M University; 2007.

650 49. Bayoh MN. Studies on the development and survival of anopheles gambiae sensu stricto at various
651 temperatures and relative humidities [Internet] [Doctoral]. Durham University; 2001 [cited 2014 Oct 15].
652 Available from: http://etheses.dur.ac.uk/4952/

653 50. Parton WJ, Logan JA. A model for diurnal variation in soil and air temperature. Agric Meteorol. 1981 Jan
654 1;23:205–16.

655 51. Paaijmans KP, Heinig RL, Seliga RA, Blanford JI, Blanford S, Murdock CC, et al. Temperature variation
656 makes ectotherms more sensitive to climate change. Glob Change Biol. 2013 Aug 1;19(8):2373–80.

657 52. Vasseur DA, DeLong JP, Gilbert B, Greig HS, Harley CDG, McCann KS, et al. Increased temperature variation
658 poses a greater risk to species than climate warming. Proc R Soc Lond B Biol Sci. 2014 Mar
659 22;281(1779):20132612.

660 53. Narasimhan R. weatherData: Get Weather Data from the Web [Internet]. 2014 [cited 2016 May 25]. Available
661 from: https://cran.r-project.org/web/packages/weatherData/index.html

662 54. Breheny P, Burchett W. visreg: Visualization of Regression Models [Internet]. 2016 [cited 2016 Jun 8].
663 Available from: https://cran.r-project.org/web/packages/visreg/index.html

664

665

666 **Figure 1**

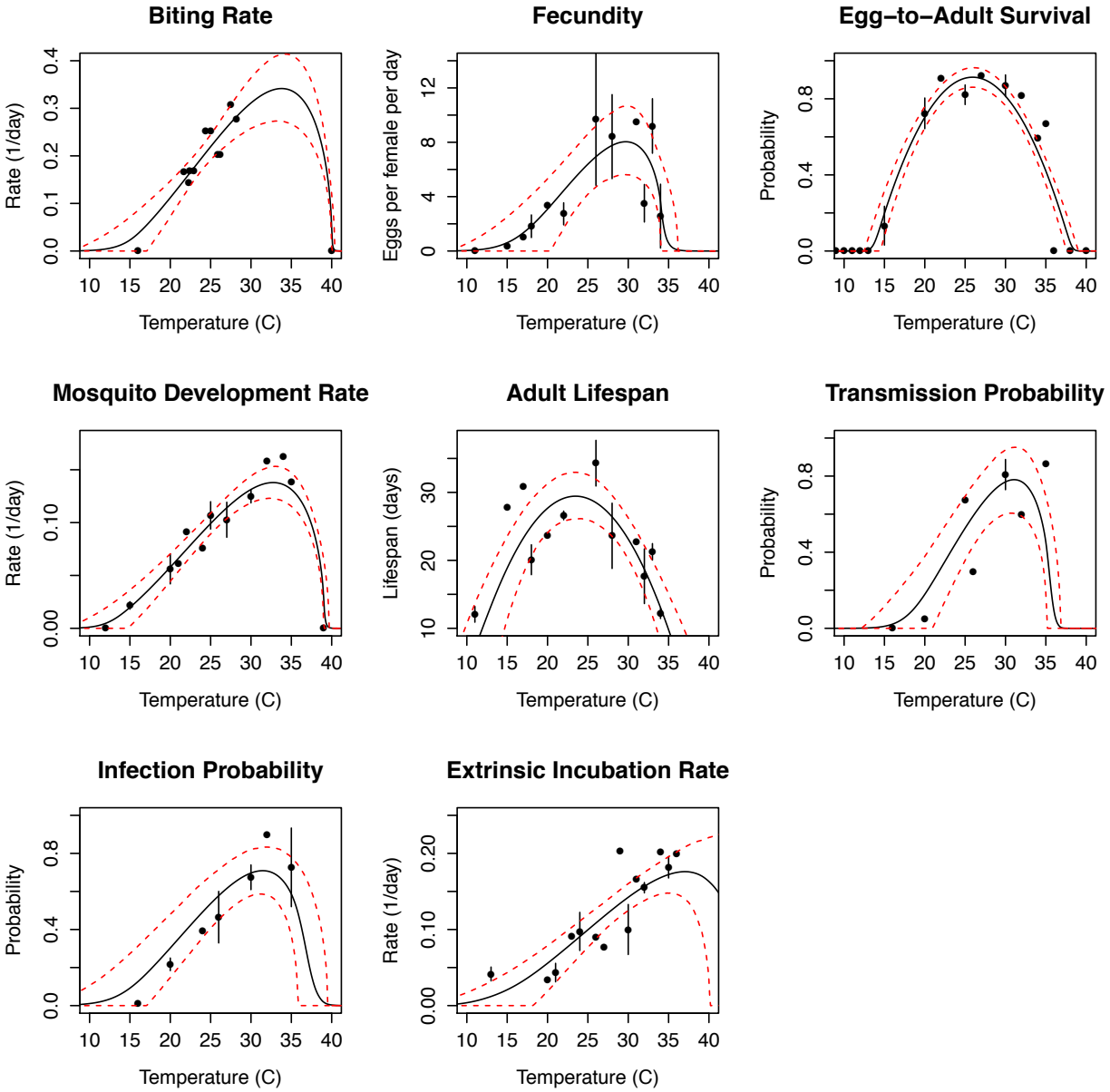

667
668

669 **Figure 2**

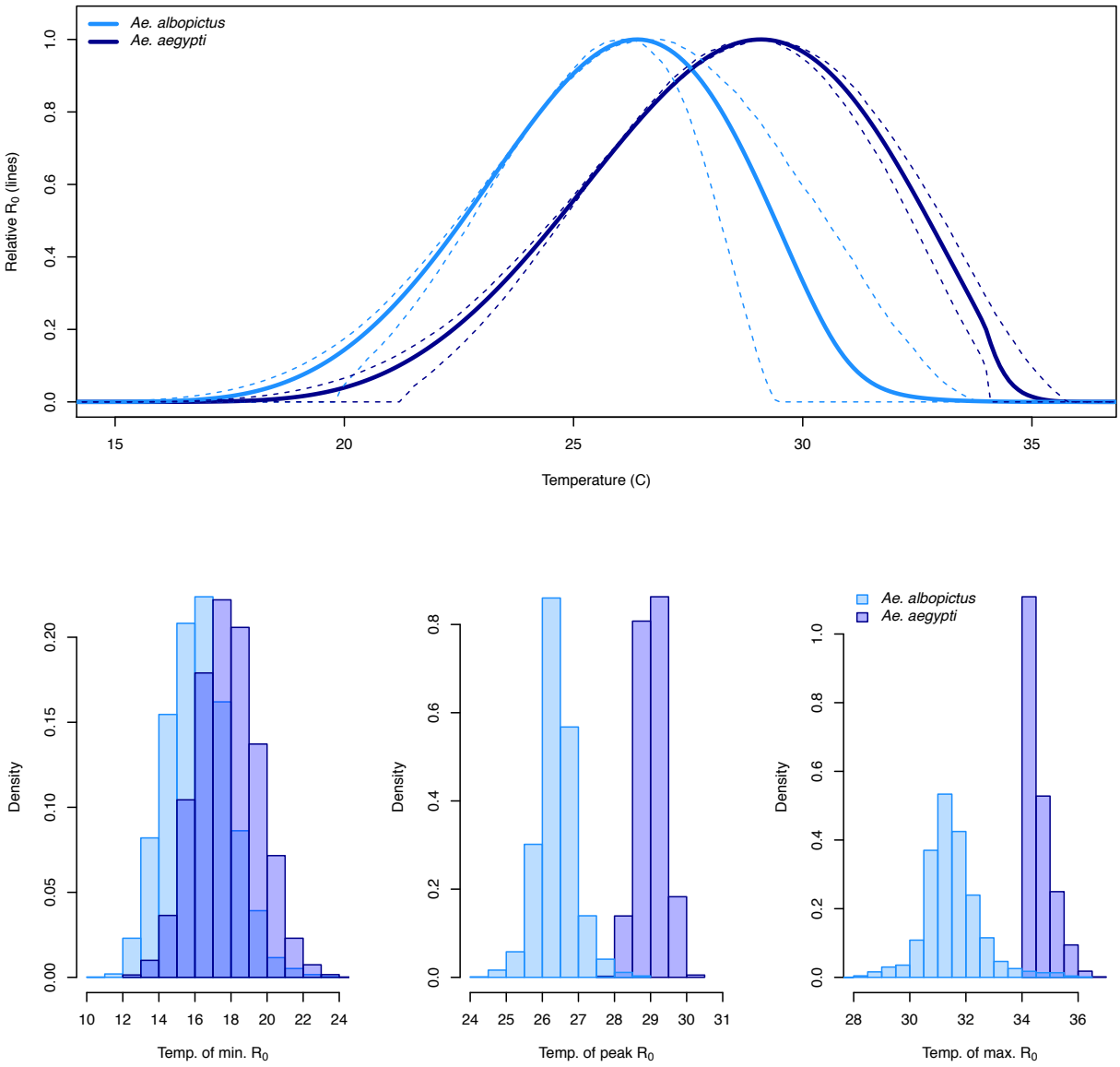

670
671

672 **Figure 3**

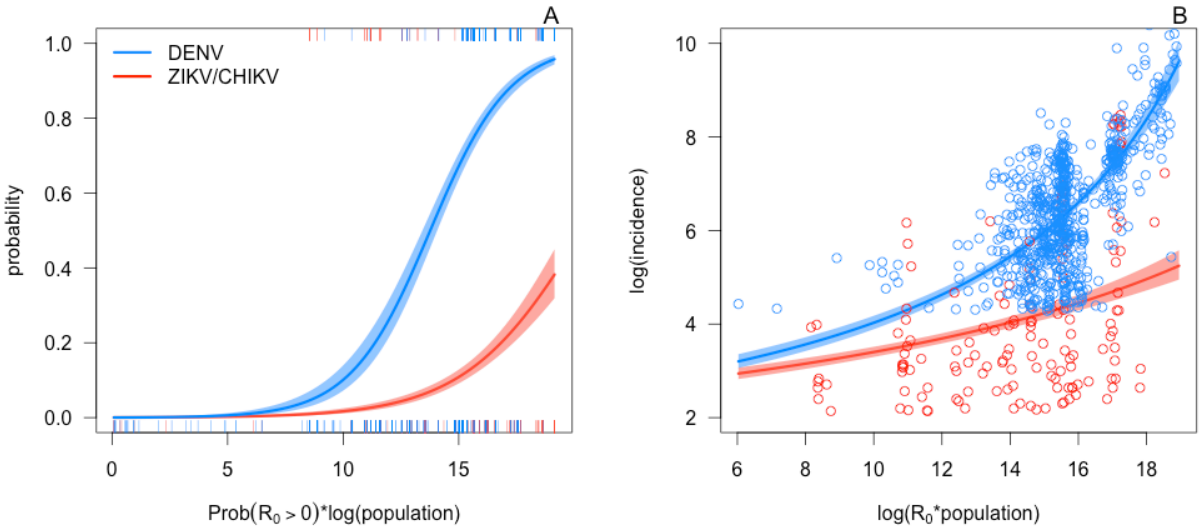

673
674

675 **Figure 4**

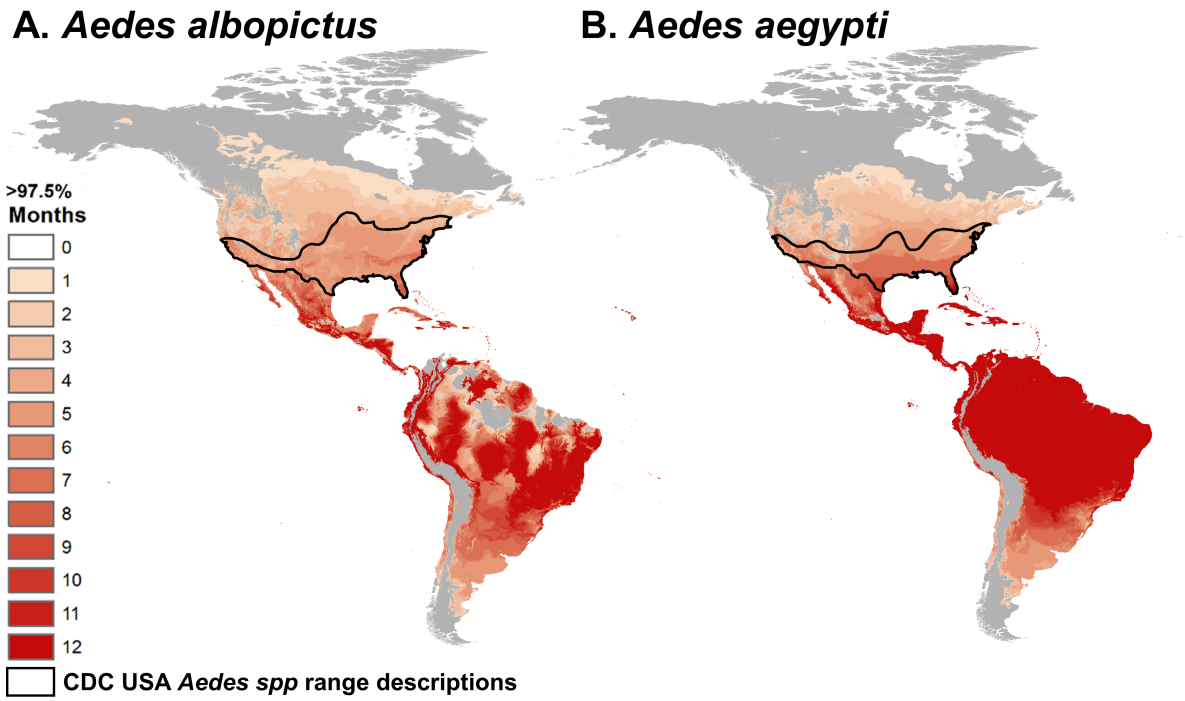

676
677